ISSN 1674-1056
http://cpb.iphy.ac.cn
http://iopscience.iop.org/cpb
中国物理 B
Chinese Physics
中国物理 Chinese Physics B

Efficient ternary organic solar cells with high absorptioncoefficient DIB-SQ as third component

Hui-Xin Qi(齐慧欣), Bo-Han Yu(余泊含), Sai Liu(刘赛), Miao Zhang(张苗), Xiao-Ling Ma(马晓玲), Jian Wang(王健), Fu-Jun Zhang(张福俊)
Citation: Chin. Phys. B . 2018, 27(5): 058802. **doi:** 10.1088/1674-1056/27/5/058802

Journal homepage: http://cpb.iphy.ac.cn; http://iopscience.iop.org/cpb

What follows is a list of articles you may be interested in

A simulation study on p-doping level of polymer host material in P3HT: PCBM bulk heterojunction solar cells

Hossein Movla, Mohammad Babazadeh
Chin. Phys. B . 2017, 26(4): 048802. **doi:** 10.1088/1674-1056/26/4/048802

Highly conductive and transparent carbon nanotube-based electrodes for ultrathin and stretchable organic solar cells

Qingxia Fan(范庆霞), Qiang Zhang(张强), Wenbin Zhou(周文斌), Feng Yang(杨丰), Nan Zhang(张楠), Shiqi Xiao(肖仕奇), Xiaogang Gu(谷孝刚), Zhuojian Xiao(肖卓建), Huiliang Chen(陈辉亮), Yanchun Wang(王艳春), Huaping Liu(刘华平), Weiya Zhou(周维亚)
Chin. Phys. B . 2017, 26(2): 028801. **doi:** 10.1088/1674-1056/26/2/028801

Sodium chloride methanol solution spin-coating process for bulk-heterojunction polymer solar cells

Tong-Fang Liu(刘统方), Yu-Feng Hu(胡煜峰), Zhen-Bo Deng(邓振波), Xiong Li(李熊), Li-Jie Zhu(朱丽杰), Yue Wang(王越), Long-Feng Lv(吕龙锋), Tie-Ning Wang(王铁宁), Zhi-Dong Lou(娄志东), Yan-Bing Hou(侯延冰), Feng Teng(滕枫)
Chin. Phys. B . 2016, 25(8): 088801. **doi:** 10.1088/1674-1056/25/8/088801

Photoinduced degradation of organic solar cells with different microstructures

Lu Chun-Xi, Yan Peng, Wang Jin-Ze, Liu Ai-Min, Song De, Jiang Chao
Chin. Phys. B . 2014, 23(8): 088803. **doi:** 10.1088/1674-1056/23/8/088803

Effective absorption enhancement in small molecule organic solar cells using trapezoid gratings

Xiang Chun-Ping, Jin Yu, Liu Jie-Tao, Xu Bin-Zong, Wang Wei-Min, Wei Xin, Song Guo-Feng, Xu Yun
Chin. Phys. B . 2014, 23(3): 038803. **doi:** 10.1088/1674-1056/23/3/038803

Efficient ternary organic solar cells with high absorption coefficient DIB-SQ as the third component*

Hui-Xin Qi(齐慧欣)[1], Bo-Han Yu(余泊含)[1], Sai Liu(刘赛)[1], Miao Zhang(张苗)[1], Xiao-Ling Ma(马晓玲)[1], Jian Wang(王健)[2,†] and Fu-Jun Zhang (张福俊)[1,‡]

[1] *Key Laboratory of Luminescence and Optical Information of Ministry of Education, Beijing Jiaotong University, Beijing* 100044, *China*
[2] *College of Physics and Electronic Engineering, Taishan University, Taian* 271021, *China*

(Received 1 January 2018; revised manuscript received 19 January 2018; published online 18 April 2018)

A series of organic solar cells (OSCs) are prepared with PTB7:$PC_{71}BM$ as the host materials and DIB-SQ as the third component. The power conversion efficienty (PCE) of OSCs can be improved from 6.79% to 7.92% by incorporating 6 wt% DIB-SQ into donors, resulting from the enhanced short circuit current density (J_{SC}) and fill factor (FF). The increased J_{SC} of the optimized ternary OSCs should be attributed to the enhanced photon harvesting of teranry active layer by incorporating DIB-SQ. Meanwhile, FF of the optimized ternary OSCs should be due to the optimied phase separation. The open circuit voltage (V_{OC}) of tenray OSCs can be maintained at a constant of 0.75 V, indicating that all photogenerated holes willl be transported along the channels formed by PTB7.

Keywords: organic solar cells, power conversion efficiency, the third component

PACS: 88.40.jr, 88.40.hj, 85.30.–z **DOI:** 10.1088/1674-1056/27/5/058802

1. Introduction

Organic solar cells (OSCs) have acheived great progress during the past years due to the rapid development of organic semiconducting materials.[1–4] The adequate photon harvesting of active layers is the prerequsite for obtianing highly efficient OSCs. To improve the photon harvesting ability and range of OSCs, two sub-cells can be connected with semi-transparnet middle electrode, named as tandem OSCs. There are some challanges to obtian highly efficient tandem OSCs: i) optimizing the thickness of sub-active layers to balance the short circuit current density (J_{SC}) of sub-cells, ii) the efficient middle electrode with proper transmissivity and high ability to collect charged carriers from the sub-cells, iii) the complementary absorption spectra of sub-active layers.[5–7] The complex and rigorous fabrication process restricts the development of tandem OSCs, especially for their real application as products. Recent years, a simple and efficient method was proposed to inherit the advantages of tandem OSCs and single layer bulk heterojunction OSCs, named as ternary OSCs.[8] The ternary OSCs were commonly prepared with two donors and one acceptor or two acceptors and one donor. The third component should have complementary absorption spectrum with host materials to improve the photon haversing of ternary active layer. Most of ternary OSCs were prepared with a narrow bandgap material to improve photon harvesting in a longer wavelength range. It is inevitable to generate some charge traps by incorporating the third component due to their differences in highest occupied molecular orbit (HOMO) and the lowest unoccupied molecular orbit (LUMO) levels among used materials. The narrow bandgap material as the third component may form some deep charge traps in the active layers due to the large energy level offsets among the used materials. The ability to transport the charges will be reduced due to the existence of charge traps induced by the incorporation of the third component. The performance of OSCs could be improved by incorporating an appropriate third component if the photon harvesting, exciton dissocation and charge transport can be balanced in ternary active layers. The different working mechansims for ternary OSCs have been reported with different donor and acceptor materials, such as energy transfer, charge transfer, parallel-linkage model and alloy-model.[9–13] The compatibility of used materials plays a key role in determining the working mechanism for ternary OSCs because intermolecular dynamic process strongly depends on the distance of intermolecules.[14] It is known that phase separation degree of used materials also influences exciton dissociation and charge transport efficiency, and the third component is also used as morphology regulator to optimize the morphologies of active layers.[15–18]

In this work, polymer polythieno[3,4-b]-thiophene / benzodithiophene (PTB7) and fullerene derivation [6,6]-phenyl-C71-butyric acid methyl ester ($PC_{71}BM$) are selected as electron donor and acceptor, respectively. Small molecule 2,4-

*Project supported by the National Natural Science Foundation of China (Grant Nos. 61675017, 61377029, and 61705161) and the National Training Program of Innovation and Entrepreneurship for Undergraduates, China (Grant No. 170170010).

†Corresponding author. E-mail: 1986.wangjian@163.com
‡Corresponding author. E-mail: fjzhang@bjtu.edu.cn

© 2018 Chinese Physical Society and IOP Publishing Ltd

bis[4-(N,N-diisobutylamino)-2,6-dihydroxyphenyl] squaraine (DIB-SQ) is used as the third component to prepare ternary OSCs. A series of ternary OSCs is prepared with PTB7:DIB-SQ:$PC_{71}MB$ as active layers, and the only difference is DIB-SQ content in donor. The bandgap of DIB-SQ is slightly larger than that of PTB7, which can improve photon harvesting in a short waveleng range. To give the more solid experimental results, the binary OSCs with PTB7:$PC_{71}BM$ as active layers are carefully optimized to achieve a maximal power conversion efficiency (PCE) of 6.86%. Based on the optimized binary OSCs, the performance of ternary OSCs can be optimized by adjsuting the DIB-SQ content in donors. The PCE of tenrary OSCs arrives to 7.92%, with an enhanced J_{SC} of 15.29 mA·cm^{-2}, a fill factor (FF) of 69.09%, and a constant open circuit voltage (V_{OC}) of 0.75 V when the DIB-SQ content is about 6 wt% in donors. The enhanced FF indicates that charge transport channels in teranry active layers could be optimized by incorporating an appropriate DIB-SQ, which may act as a morphology regulator for obtaining ideal phase separation in the ternary active layers. About 15% PCE improvement can be obtained by incorporating 6 wt% DIB-SQ as the third component, which is mainly attributed to the enhanced photon havesting and optimized phase separation in the optimized ternary active layers.

2. Experiment

The patterned indium tin oxide (ITO) coated glass substrates (15 Ω per square) were cleaned via sequential sonication in detergent, deionized water and ethanol. Then the cleaned ITO substrates were dried by high-purity nitrogen and treated by oxygen plasma for 1 min to improve their work function and clearance. Subsequently, poly(3,4-ethylenedioxythiophene):poly (styrene sulfonate) (PEDOT:PSS, purchased from H.C. Starck co. Ltd.) was spin-coated on ITO substrates at 5000 RPM for 40 s and dried at 150 °C for 10 min in atmospheric air. Then ITO substrates coated with PEDOT:PSS films were transferred into a high-purity nitrogen-filled glove box. The used materials PTB7, DIB-SQ and $PC_{71}BM$ were purchased from Luminescence Technology Corp. and 1-Material. The mixed PTB7:$PC_{71}BM$ (1:1.5, wt/wt) and DIB-SQ:$PC_{71}BM$ (1:1.5, wt/wt) powder were separately dissolved in chlorobenzene with 3 vol% 1,8-diiodooctane (DIO) to prepare 25 mg/mL binary blend solutions. Ternary blend solutions of $PTB7_{1-x}$:DIB-SQ_x:$PC_{71}BM_{1.5}$ (x represents DIB-SQ content in donors) were prepared by mixing binary solutions with different volume ratios. The mixed solutions were spin-coated onto the PEDOT:PSS/ITO substrates at 1500 RPM for 40 s to prepare the active layers. The conjugated poly[(9,9-bis(3-(N,N-dimethylamino)-propyl)-2,7-fluorene)-alt-2,7-(9,9-dioctylfluorene)] (PFN) was dissolved in methanol with the addition of 0.25 vol% acetic acid to prepare a 0.2 mg/mL solution. Then the prepared PFN solutions were spin-coated onto the active layers at 3000 RPM for 40 s. Finally, aluminum (Al) electrode was deposited by thermal evaporation. The active area was approximately 3.8 mm^2, which was defined by the overlapping area of ITO anode and Al cathode.

The current density–voltage (J–V) characteristics were measured by a Keithley 2400 unit in a high-purity nitrogen-filled glove box. The AM 1.5G irradiation was provided by an XES-40S2 (SAN-EI ELECTRIC Co., Ltd) solar simulator (AAA grade, 70×70 mm^2 photobeam size) with a light intensity of 100 mW/cm^2. The external quantum efficiency (EQE) spectra were measured by a Zolix Solar Cell Scan 100. The absorption spectra of films were measured with a Shimadzu UV-3101 PC spectrometer. Transmission electron microscopy (TEM) images were obtained by a JEOL JEM-1400 transmission electron microscope operated at 80 kV. The chemical structures of used materials, schematic diagram of device structure and energy level diagram of used materials are shown in Fig. 1.

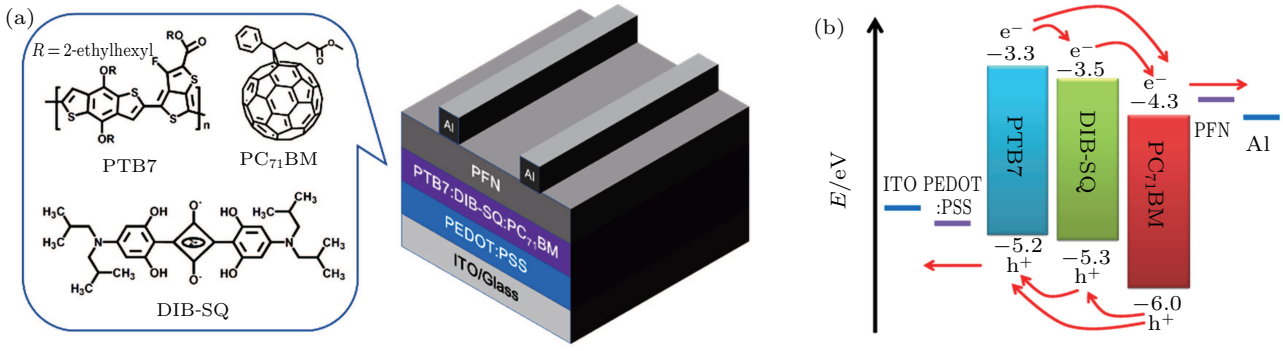


Fig. 1. (color online) (a) Chemical structures of used materials and the schematic diagram of device structure, and (b) energy level diagram of used materials and the arrows represent charge transport direction.

3. Results and discussion

A series of ternary OSCs is fabricated with PTB7:DIB-SQ as donors and $PC_{71}BM$ as acceptor, and the only difference is DIB-SQ content ($x = 0$, 3%, 6%, 9%, 12%, 100% weight ratios) in donors. The small molecule DIB-SQ is selected as the second donor to enhance photon harvesting and optimize morphology of active layers. The absorption spectra of neat PTB7, DIB-SQ and $PC_{71}BM$ films are measured and shown in Fig. 2(a). It is apparent that PTB7 exhibits a broad photon harvesting range from 550 nm to 750 nm and DIB-SQ exhibits a relatively narrow photon harvesting range from 620 to 680 nm. The $PC_{71}BM$ has strong ability to harvest photons in a short wavelength range and long tail in long wavelength range. The absorption spectra of blend films with different DIB-SQ content are measured and are shown in Fig. 2(b). The absorption intensities of blend films can be markedly improved from 620 nm to 680 nm with the increase of DIB-SQ content in donors, which should be attributed to the large absorption coefficient of DIB-SQ. The absorption intensity of blend film slightly decreases from 450 nm to 600 nm with the increase of DIB-SQ content in donors due to the reduced PTB7 content. The more photon harvesting of active layers should be obtained in the whole spectral range by optimizing DIB-SQ content, which is the prerequisite for preparing efficient OSCs.

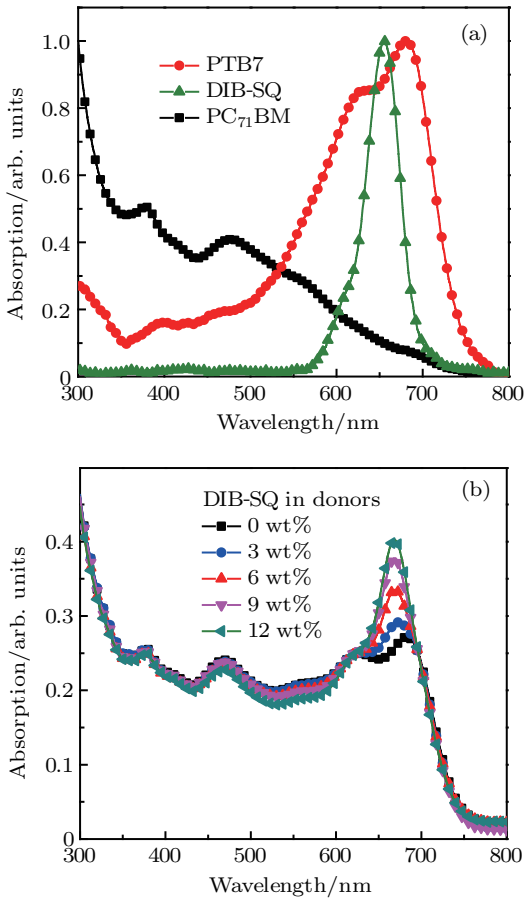


Fig. 2. (color online) (a) Normalized absorptions of the used materials in thin films, and (b) absorption spectra of blend films with different DIB-SQ content in donors.

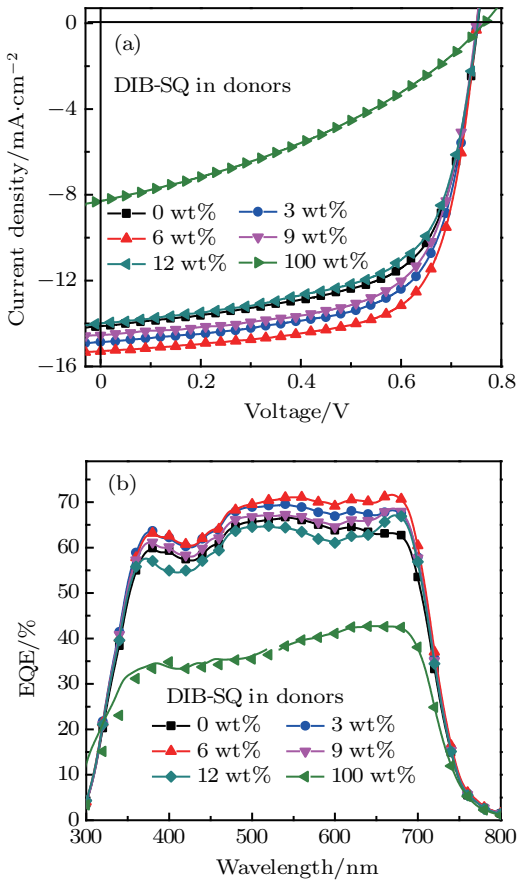


Fig. 3. (color online) (a) The J–V curves of OSCs with different DIB-SQ content in donors under AM 1.5G illumination with light intensity of 100 mW·cm^{-2}, and (b) EQE spectra of the corresponding OSCs.

The current density–voltage (J–V) curves of all OSCs are measured under AM 1.5G illumination with a light intensity of 100 mW/cm^2 as shown in Fig. 3(a). The PTB7:$PC_{71}BM$ based binary OSCs exhibit a PCE of 6.86% with a J_{SC} of 14.12 mA·cm^{-2}, a V_{OC} of 0.75 V and an FF of 64.83%. The DIB-SQ:$PC_{71}BM$ based OSCs exhibit a relatively low PCE of 2.29%, with a J_{SC} of 8.28 mA·cm^{-2}, a V_{OC} of 0.77 V, and rather low FF of 35.92%. The relatively low J_{SC} of DIB-SQ:$PC_{71}BM$ based OSCs can be well explained due to the narrow absorption spectrum of DIB-SQ and inefficient charge transport and collection. The DIB-SQ:$PC_{71}BM$ based OSCs exhibit a rather low FF due to the discontinuous charge transport channels resulting from excessive phase separation. Both J_{SC} and FF of ternary OSCs can increase and then decrease with the increase of DIB-SQ content in donors, and the improvements of J_{SC} and FF should be attributed to the enhanced photon harvesting and optimized phase separation. The decreasing of J_{SC} and FF should be due to the excessive phase separation, which can be confirmed from the DIB-SQ:$PC_{71}BM$ binary OSCs. The V_{OC} of ternary OSCs can be maintained at a constant of 0.75 V. As shown in Fig. 2(b), the cascade energy levels among PTB7, DIB-SQ and $PC_{71}BM$ provide efficient charge transport channels in ternary OSCs. The PTB7 and DIB-SQ exhibit the similar HOMO energy levels of −5.2 eV and −5.3 eV, which is beneficial for efficient

hole transfer from the HOMO of DIB-SQ onto the HOMO of PTB7. In ternary OSCs, photogenerated electrons or holes will be mainly transported along the channels formed by $PC_{71}BM$ or PTB7, which can well explain the constant V_{OC} values for ternary OSCs with different DIB-SQ content in donors. It is known that the FF of OSCs strongly depends on shunt resistance (R_{SH}) and series resistance (R_S), which can be calculated according to the reciprocal of J–V curve slope under the short circuit or open circuit condition, respectively.[19,20] The reduced R_S and increased R_{SH} should be beneficial to charge transport and collection, leading to the improved FF of OSCs. The EQE spectra of all OSCs are measured and are shown in Fig. 3(b). According to the EQE spectra, the calculated J_{SC} values of ternary OSCs are slightly less than the measured values with a deviation of less than 2% due to the cells without encapsulation for EQE measurement. It is apparent that the EQE values can be slightly improved in the whole spectral range by incorporating small amount of DIB-SQ, which should be attributed to the optimized morphology for better exciton dissociation, charge transport and collection in the corresponding ternary OSCs. When DIB-SQ content is larger than 6 wt% in donors, the EQE value of OSCs will decrease due to the disrupted phase separation in the ternary active layers. All the key parameters of OSCs are summarized in Table 1.

Table 1. Key photovoltaic parameters of PSCs with different DIB-SQ content in donors.

DIB-SQ/wt%	J_{SC}/mA·cm^{-2}	Cal. J_{SC}/mA·cm^{-2}	V_{OC}/V	FF/%	PCE/%		R_S/Ω·cm^2	R_{SH}/Ω·cm^2
					Best	Avg.		
0	14.12	13.87	0.75	64.83	6.86	6.76	6.1	577
3	14.86	14.66	0.75	67.01	7.47	7.30	5.3	633
6	15.29	15.05	0.75	69.09	7.92	7.85	4.9	709
9	14.55	14.32	0.75	66.12	7.22	7.16	5.8	685
12	14.01	13.73	0.75	63.30	6.65	6.54	6.3	495
100	8.28	8.22	0.77	35.92	2.29	2.15	69.9	356

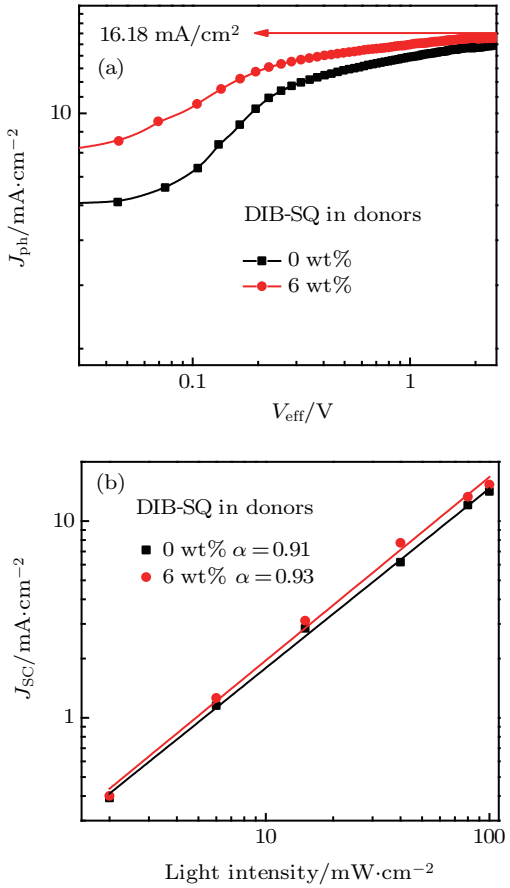


Fig. 4. (color online) (a) The J_{ph}–V_{eff} curves of the optimized ternary and PTB7:$PC_{71}BM$ based PSCs, and (b) J_{SC} versus light intensity of the optimized ternary and PTB7:$PC_{71}BM$ based PSCs.

To further clarify the underlying reason why the appropriate DIB-SQ incorporation can lead to the performance improvement of OSCs, the J–V curves of OSCs are measured in dark and under light illumination, separately. The photocurrent density (J_{ph}) can be calculated from the equation: $J_{ph} = J_l - J_d$, where J_l and J_d are the current densities under 100 mW/cm^2 light illumination and in dark conditions. Figure 4(a) shows the J_{ph} dependence on effective voltage ($V_{eff} = V_0 - V_a$) of OSCs, where V_0 is the voltage for $J_{ph} = 0$, and V_a is the applied bias.[21] The exciton dissociation and charge collection efficiency can be evaluated according to the ratios of J_{ph} to the saturation photocurrent density (J_{sat}), i.e., (J_{ph}/J_{sat}) under short circuit and maximal power output conditions, respectively.[22–24] The J_{sat} should be mainly determined by photon harvesting of active layers, which can be described as $J_{sat} = qLG_{max}$, where q is the elementary charge and L is the thickness of active layers, G_{max} is the maximum exciton generation rate. The J–V curves of DIB-SQ:$PC_{71}BM$ based OSCs cannot be obtained under large bias due to the fact that it easily breaks down. The optimized ternary OSCs exhibit a larger J_{sat} of 16.18 mA·cm^{-2} and a larger G_{max} of 0.84×10^{28} m^{-3}·s^{-1} compared with 15.45 mA·cm^{-2} and 0.80×10^{28} m^{-3}·s^{-1} for PBT7:$PC_{71}BM$ based OSCs, indicating that the photon harvesting should be improved in the optimized ternary active layers. The J_{ph} under short circuit and maximal power output conditions, J_{sat} and the ratios between the optimized ternary and PTB7:$PC_{71}BM$ based OSCs are summarized in Table 2. It is apparent that the J_{ph}/J_{sat} values of the optimized ternary OSCs are larger than those of PTB7:$PC_{71}BM$ based OSCs, further indicating that efficiency

of exciton dissociation, charge transport and collection can be improved in the optimized ternary OSCs compared with in the binary OSCs. The relationship between J_{SC} and P_{light} can be expressed as $J_{SC} \propto P^{\alpha}$.[25–27] As shown in Fig. 4(b), the fitted α value is approximately 0.91 or 0.93 for binary or the optimized ternary PSCs, respectively. The relatively large α value of 0.93 suggests the less bimolecular recombination in the optimized ternary OSCs.

To further clarify the effect of DIB-SQ content in donors on charge transport in active layers, charge mobility in active layers with different DIB-SQ content is measured by using space charge limited current (SCLC) method.[28–30] The electron-only and hole-only devices are fabricated with the structures of ITO/ZnO/active layers/PFN/Al and ITO/PEDOT:PSS/active layers/MoO_3/Ag, respectively. The active layers of electron-only and hole-only devices are the sameas those of corresponding OSCs. The $\ln(Jd^3/V^2) - (V/d)^{0.5}$ curves of hole-only and electron-only devices are shown in Fig. 5. The hole mobility (μ_h) and electron mobility (μ_e) in the active layers monotonically decrease with the increase of DIB-SQ content. The μ_h/μ_e value of 1.15 for active layers with 6 wt% DIB-SQ is closest to unity, indicating that the hole and electron transport become more balanced in the ternary active layers. The μ_h/μ_e values deviate from unity for the active layer with DIB-SQ content more than 6 wt%, indicating the unbalanced charge transport in the ternary active layers with higher DIB-SQ content in donors. The variation of μ_h/μ_e value can well explain the dependence of FF of ternary OSCs on DIB-SQ content in donors.

Table 2. J_{ph}, J_{sat}, G_{max}, and J_{ph}/J_{sat} values of optimized ternary and PTB7:PC_{71}BM based OSCs.

DIB-SQ content/wt%	J_{ph}[a]/mA·cm^{-2}	J_{ph}[b]/mA·cm^{-2}	J_{sat}/mA·cm^{-2}	G_{max}/m^{-3}·s^{-1}	J_{ph}/J_{sat}[a]/%	J_{ph}/J_{sat}[b]/%
0	14.12	11.74	15.45	0.80×10^{28}	91.4	76.0
6	15.29	13.04	16.18	0.84×10^{28}	94.5	80.6

[a]short-circuit condition, [b]maximal power output condition.

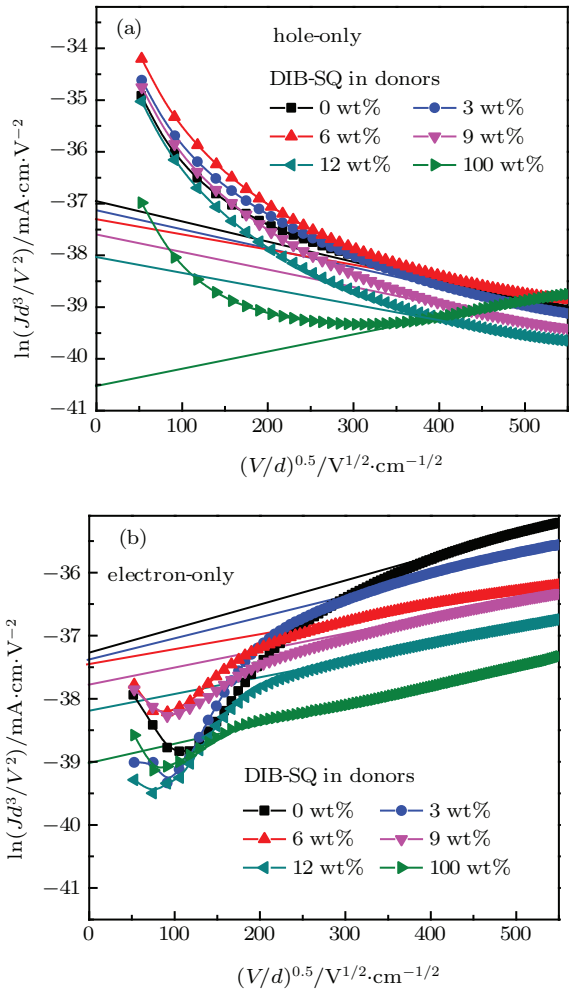


Fig. 5. (color online) Plots of $\ln(Jd^3/V^2)$ versus $(V/d)^{0.5}$ of (a) hole-only devices and (b) electron-only devices.

Table 3. Values of μ_h and μ_e and their ratios (μ_h/μ_e) in active layers with different DIB-SQ content in donors.

DIB-SQ/wt%	μ_h/cm^2·V^{-1}·s^{-1}	μ_e/cm^2·V^{-1}·s^{-1}	μ_h/μ_e
0	2.86×10^{-4}	2.12×10^{-4}	1.35
3	2.51×10^{-4}	1.97×10^{-4}	1.27
6	2.12×10^{-4}	1.84×10^{-4}	1.15
9	1.57×10^{-4}	1.32×10^{-4}	1.19
12	1.05×10^{-4}	0.85×10^{-4}	1.24
100	8.63×10^{-6}	3.87×10^{-5}	0.22

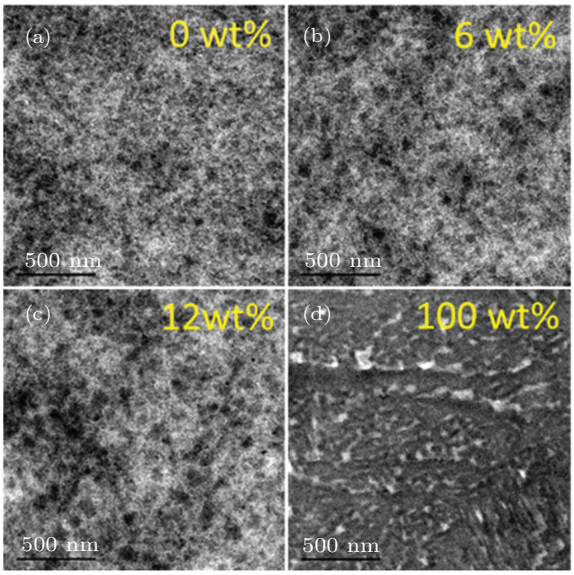


Fig. 6. (color online) TEM images of blend films with different DIB-SQ content in donors. (a) 0 wt%, (a) 6 wt%, (c) 12 wt%, and (d) 100 wt%.

Transmission electron microscopy (TEM) is used to investigate the effect of DIB-SQ content in donors on the mor-

phology of blend films- as shown in Fig. 6. Obviously, the fibrillar features can be observed from the PTB7:$PC_{71}BM$ blend films. Some large aggregations can be observed from the DIB-SQ:$PC_{71}BM$ blend films, which may restrict exciton dissociation and charge transport in the active layers. The excessive phase separation results in the low PCE of DIB-SQ:$PC_{71}BM$ based OSCs. The morphologies of ternary active layers can be slightly adjusted by incorporating DIB-SQ, the optimized morphology may be beneficial to exciton dissociation and charge transport for the performance improvement. The enhanced FF of the optimized ternary OSCs can also confirm the optimized morphology in the ternary active layers. The PCE improvement of ternary OSCs should be mainly attributed to the enhanced photon harvesting and the optimized morphology of the ternary active layers with 6 wt% DIB-SQ in donors.

4. Conclusions

In this work, a series of ternary OSCs with different DIB-SQ content in donors has been prepared. The PCE of ternary OSCs is improved to 7.92% by incorporating 6 wt% DIB-SQ into donors, resulting from the enhanced J_{SC} of 15.29 mA·cm^{-2} and FF of 69.09%. The V_{OC} of ternary OSCs can be kept at a constant of 0.75 V, indicating that all photogenerated holes will be transported along the channels formed by PTB7. About 15% PCE improvement of ternary OSCs should be mainly attributed to the enhanced photon harvesting and the optimized morphology by incorporating appropriate DIB-SQ. The experimental results further confirm the ternary strategy as an efficient method to improve the performance of OSCs.

References

[1] Zhao W, Li S, Yao H, Zhang S, Zhang Y, Yang B and Hou J 2017 *J. Am. Chem. Soc.* **139** 7148

[2] Bin H, Zhang Z G, Gao L, Chen S, Zhong L, Xue L, Yang C and Li Y 2016 *J. Am. Chem. Soc.* **138** 4657

[3] Xue L, Yang Y, Xu J, Zhang C, Bin H, Zhang Z G, Qiu B, Li X, Sun C and Gao L 2017 *Adv. Mater.* **29** 1703344

[4] Chen S, Liu Y, Zhang L, Pcy C, Wang Z, Zhang G, Ma W and Yan H 2017 *J. Am. Chem. Soc.* **139** 6298

[5] Ameri T, Dennler G, Lungenschmied C and Brabec C J 2009 *Energy Environ. Sci.* **2** 347

[6] Dou L, You J, Yang J, Chen C C, He Y, Murase S, Moriarty T, Emery K, Li G and Yang Y 2012 *Nat. Photonics* **6** 180

[7] Gevaerts V S, Furlan A, Wienk M M, Turbiez and Janssen R A 2012 *Adv. Mater.* **24** 2130

[8] An Q, Zhang F, Zhang J, Tang W, Deng Z and Hu B 2016 *Energy Environ. Sci.* **9** 281

[9] Huang J S, Goh T, Li X, Sfeir M Y, Bielinski E A, Tomasulo S, Lee M L, Hazari N and Taylor A D 2013 *Nat. Photonics* **7** 479

[10] Honda S, Yokoya S, Ohkita H, Benten H and Ito S 2011 *J. Phys. Chem. C* **115** 11306

[11] Zhang M, Zhang F, Wang J, An Q and Sun Q 2015 *J. Mater. Chem. C* **3** 11930

[12] Wang Z, Zhang Y, Zhang J, Wei Z and Ma W 2016 *Adv. Energy Mater.* **6** 1502456

[13] An Q, Zhang F, Li L, Wang J, Sun, Q, Zhang J, Tang W and Deng Z 2015 *ACS Appl. Mater. Interfaces* **7** 3691

[14] Su W, Fan Q, Guo X, Meng X, Bi Z, Ma W, Zhang M and Li Y 2017 *Nano Energy* **38** 510

[15] Zhang M, Zhang F, An Q, Sun Q, Wang W, Ma X, Zhang J and Tang W 2017 *J. Mater. Chem. A* **5** 3589

[16] Gasparini N, Jiao X, Heumueller T, Baran D, Matt G J, Fladischer S, Spiecker E, Ade H, Brabec C J and Ameri T 2016 *Nat. Energy* **1** 16118

[17] Zhang Y, Deng D, Lu K, Zhang J, Xia B, Zhao Y, Fang J and Wei Z 2015 *Adv. Mater.* **27** 1071

[18] Ma X, Zhang F, An Q, Sun Q, Zhang M, Miao J, Hu Z and Zhang J 2017 *J. Mater. Chem. A* **5** 13145

[19] Jao M H, Liao H C and Su W F 2016 *J. Mater. Chem. A* **4** 5784

[20] Gupta D, Mukhopadhyay S and Narayan K S 2010 *Sol. Energy Mater. Sol. Cells* **94** 1309

[21] Blom P W M, Mihailetchi V D, Koster L J A and Markov D E 2007 *Adv. Mater.* **19** 1551

[22] Lu L, Xu T, Chen W, Landry E S and Yu L 2014 *Nat. Photonics* **8** 716

[23] He Z, Zhong C, Huang X, Wong W Y, Wu H, Chen L, Su S and Cao Y 2011 *Adv. Mater.* **23** 4636

[24] Ma X, Mi Y, Zhang F, An Q, Zhang M, Hu Z, Liu X, Zhang J and Tang W 2018 *Adv. Energy Mater.* **8** 1702854

[25] Kyaw A K, Wang D H, Gupta V, Leong W L, Ke L, Bazan G C and Heeger A J 2013 *ACS Nano* **7** 4569

[26] Riedel I, Parisi J, Dyakonov V, Lutsen L, Vanderzande D and Hummelen J C 2004 *Adv. Funct. Mater.* **14** 38

[27] Lu L, Chen W, Xu T and Yu L 2015 *Nat. Commun.* **6** 7327

[28] Cha H, Chung D S, Bae S Y, Lee M J, An T K, Hwang J, Kim K H, Kim Y H, Choi D H and Park C E 2013 *Adv. Funct. Mater.* **23** 1556

[29] Cui C, Guo X, Min J, Guo B, Cheng X, Zhang M, Brabec C J and Li Y 2015 *Adv. Mater.* **27** 7469

[30] Zhang M, Gao W, Zhang F, Mi Y, Wang W, An Q, Wang J, Ma X, Miao J, Hu Z, Liu X, Zhang J and Yang C 2018 *Energy Environ. Sci.* DOI: 10.1039/C8EE00215K